RESEARCH PAPER

Effect of Pre-Cold Deformation and Welding Current Mode on Mechanical Properties and Microstructure of GTAWed Nimonic 80A Superalloy

Amirreza Bali Chalandar[1,2], Amirreza Farnia[1,2,*], Hamidreza Najafi[1,2], Hamidreza Jafarian[3]

* *a.farnia@srbiau.ac.ir*

[1] Department of Materials Engineering, Science and Research Branch, Islamic Azad University, Tehran, Iran
[2] Department of Advanced Materials & Processing, Research and Development of Engineering Materials Research Center, Science and Research Branch, Islamic Azad University, Tehran, Iran
[3] School of Metallurgy and Materials Engineering, Iran University of Science and Technology (IUST), Tehran, Iran

Received: November 2024 **Revised: February 2025** **Accepted: March 2025**
DOI: 10.22068/ijmse.3821

Abstract: *This study investigates the microstructural evolution and variations in the mechanical properties of pre-cold-worked Nimonic 80A superalloy, subjected to two levels of deformation (25% and 50%) and welded via Gas Tungsten Arc Welding (GTAW) and Pulsed Current Gas Tungsten Arc Welding (PCGTAW) techniques using ER309L filler wire. The objective is to evaluate the effect of the initial microstructure on the welding behavior of Nimonic 80A and compare the weldments produced using GTAW and PCGTAW. Microstructural characterization was conducted using optical microscopy (OM), scanning electron microscopy (SEM), and X-ray diffraction (XRD). XRD analysis demonstrated that the welding pulsed current mode, compared to the continuous current mode and at equal heat input, led to a refined microstructure, suggesting improved welded mechanical properties of the weld. It also showed a potential reduction in grain refinement with a higher level of cold work. Tensile testing demonstrated that fractures consistently occurred within the weld zone (WZ), with the PCGTAW sample achieving the highest tensile strength (766 MPa). Microhardness analysis indicated a notable reduction in hardness within the heat-affected zone (HAZ) and WZ, particularly in the 50% pre-cold worked sample. However, PCGTAW retained higher hardness due to its refined microstructure. The weld metal primarily consisted of an austenitic microstructure characterized by dendrites and interdendritic precipitates. Microstructural analysis revealed that welding induced significant changes in the weldment, with the PCGTAW sample exhibiting a more uniform microstructure and smoother transitions at the weld interface. Fractography confirmed ductile fracture in all specimens, with smoother and more uniformly distributed dimples in the PCGTAW sample. These findings highlight the advantages of pulsed current welding in optimizing the mechanical performance of Nimonic 80A welds and suggest its potential application in industries requiring superior weld quality.*

Keywords: *Nimonic 80A superalloy, GTAW welding, Pre-cold worked, Initial microstructure, PCGTAW process.*

1. INTRODUCTION

Nimonic 80A, a precipitation-hardened nickel-chromium superalloy, has found widespread applications in the aerospace, power generation, and chemical processing industries due to its exceptional high-temperature strength, corrosion resistance, and creep resistance [1]. The strengthening of this alloy is highly dependent on its microstructure, which is influenced by factors such as grain size, the type and distribution of precipitates at grain boundaries, and the volume fraction of γ' precipitates within the γ matrix [2, 3]. Welding Nimonic 80 presents significant challenges due to its sensitivity to heat-affected zone (HAZ) cracking and the impact of welding-induced microstructural changes on performance. Addressing these challenges is crucial for ensuring the reliability and longevity of components subjected to high thermal and mechanical stresses [4, 5]. Gas Tungsten Arc Welding (GTAW) is a widely used joining technique for Nimonic 80A components, as it produces high-quality welds with minimal distortion [1, 6].

GTAW is a well-established method for producing high-quality welds with minimal defects [7]. Evaluating this process with different fillers helps identify the most suitable method for specific applications, balancing weld quality, efficiency, and material properties. Pre-weld deformation, such as cold working, induces grain refinement and promotes grain orientations within the alloy. These microstructural changes have been shown to significantly influence the mechanical properties, potentially affecting the alloy's weldability [8, 9]. On the other hand, Pulsed Current Gas Tungsten Arc Welding (PCGTAW) techniques, characterized by peak and base currents, also play a significant role in the welding process. Pulsed current welding provides better control of heat input and

[DOI: 10.22068/ijmse.3821]

enhances the appearance and properties of the weld bead [10-12]. The peak current influences the amount of heat generated, while the base current affects the stability of the weld pool and the formation of microstructural features. Investigating how these current parameters impact the microstructural evolution, tensile strength, hardness, and other mechanical properties of the weld can lead to optimized welding practices and enhanced performance of Nimonic 80 superalloy joints [13].

During the GTAW process, the weld metal and the heat-affected zone (HAZ) of Nimonic 80A undergo complex thermal cycles, which can significantly alter the microstructure, including grain refinement, the dissolution of strengthening precipitates, and the formation of new phases. These microstructural changes can, in turn, affect the mechanical properties of the welded joint, such as tensile strength, hardness, and impact toughness [14].

Recent studies have explored the microstructural and mechanical properties of various welding processes. Plasma arc welding of Nimonic 80A resulted in cellular dendritic structures and secondary precipitates in the weld zone, with lower strength compared to the base metal [15]. In a related study, Zhang et al. [16] used electron backscatter diffraction (EBSD) to analyze the microstructure evolution and aging behavior of electron beam welded Nimonic 80A after heat treatment. Their findings highlighted the importance of post-weld heat treatment in modifying the microstructure and improving the mechanical properties of the welded joint. Subramani et al. [13] reported that welding the nickel-based superalloy 686 using the PCGTAW method resulted in a more refined microstructure and decreased microsegregation of alloying elements in the weld zone. This improvement enhanced the metallurgical and mechanical properties of the alloy in comparison to the traditional GTAW method. Atapek et al. [17] investigated the mechanical and corrosion properties of C-276 Hastelloy welded joints using the GTAW technique. In their study, C-276 Hastelloy was welded using a continuous current in the GTAW process with an ERNiCrMo-4 filler metal. The results demonstrated that the impact toughness values in the HAZ were higher than those in the weld metal.

Keienburg et al. [18] explored the repair process of turbine blades made from alloy 80A by employing Tungsten Inert Gas (TIG) welding with Inconel 62 filler wire. Their findings revealed the formation of significant cracks at the fusion zone's weld interface. However, they also discovered that integrating a piece of Inconel 625 into alloy 80A using Inconel 625 filler wire effectively minimized these cracks, reducing them to microcracks. Similarly, Xu et al. [19] examined the microstructural changes in alloy 80A after heat treatment. They noted that $M_{23}C_6$ chromium-rich carbides tend to segregate at grain boundaries, and this localized accumulation of blocky $M_{23}C_6$ carbides negatively impacts the mechanical properties of the alloy. Manikandan and Sivakumar et al. [3] investigated the impact of different cooling rates on the segregation of alloying elements in the fusion zone of alloy 718. Their study revealed that applying a high cooling rate, achieved through the current pulsing mode, significantly reduced element segregation in the fusion zone. A comparative analysis by Srikanth and Manikandan [11] examined alloy 600 welded using GTAW and PCGTAW with three different filler wires. Their research concluded that the PCGTAW method yielded a more refined microstructure with lower microsegregation levels than conventional GTAW. Additionally, using ERNiCrMo-3 filler wire containing Nb and Mo facilitated the formation of Nb or Mo carbides (MC) rather than Cr carbides, which enhanced the alloy's mechanical performance. Furthermore, Devendranath Ramkumar et al. [20] the metallurgical and mechanical properties of alloy X750 welded using two different filler wires were assessed. Their results demonstrated that the absence of chromium precipitates and a minimal degree of Mo segregation at grain boundaries contributed to improved mechanical properties. Since both alloy 600 and alloy X750 belong to the Ni-Cr alloy system, which shares similarities with alloy 80A, similar mechanical and structural enhancements can be anticipated in alloy 80A under comparable conditions.

Subramani et al. [21] investigated the effect of hot corrosion on PCGTAW aerospace-grade alloy 80A under high-temperature molten salt environments. Their findings demonstrated that PCGTAW exhibited superior corrosion resistance compared to conventional GTAW due to grain refinement and the formation of protective oxides such as Cr_2O_3, NbO, and $NiCr_2O_4$. The study

[DOI: 10.22068/ijmse.3821]

highlights the potential of PCGTAW in enhancing the durability of high-temperature components, making it a promising technique for improving the longevity of aerospace and turbine materials. The importance of investigating the welding of Nimonic 80 cannot be overstated, given its widespread application in demanding environments where joint integrity is paramount. The critical factors affecting the quality of weldments are the influence of initial microstructure, pre-cold working, and welding current mode on GTAW and PCGTAW outcomes. Cold-rolled Nimonic 80 sheets exhibit distinct mechanical properties and microstructural characteristics compared to annealed counterparts. The initial microstructure affects how the material responds to welding, influencing the formation of the weld metal, HAZ, and overall joint properties. No studies have compared the effects of pulsed and continuous current modes in the GTAW process on Nimonic 80A pre-cold worked in different amounts. Understanding the impact of pre-weld processing conditions and welding current mode on microstructural evolution, tensile strength, hardness, and other mechanical properties of the weld can lead to optimized welding practices and enhanced performance of Nimonic 80 superalloy joints. The effect of pre-cold working and PCGTAW on the microstructure and mechanical properties of weldments is investigated in this research. The findings can be directly applied in industries without requiring significant modifications to existing welding processes, enabling the production of defect-free welds during fabrication or refurbishing.

2. EXPERIMENTAL PROCEDURES

2.1. Materials and Sample Preparation

The Nimonic 80A alloy, used as the base material, was obtained as sheets with a thickness of 4 mm in the cold-rolled state in two different pre-cold worked amounts of 25% and 50%. ER309L filler, with a diameter of 1.2 mm, was selected as the filler material. The chemical composition of the base metal and the filler was determined using Optical Emission Spectroscopy (OES), with the results presented in Table 1. Acid pickling was performed on the plates to remove surface impurities such as rust. Before welding, the sheets were cleaned with acetone to eliminate oil, dirt, and other contaminants. A single V-groove configuration with an included angle of 70° was prepared on the sheets before welding, as shown in Fig. 1.

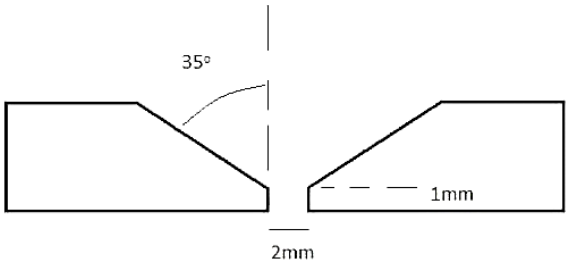

Fig. 1. Schematic of the joint design

2.2. Welding Process

The machined sheets were securely clamped to fixtures to prevent distortion during welding. Manual GTAW was conducted using an argon flow rate of 15 L/min and direct current electrode negative (DCEN) polarity, utilizing a KEMPI DWE 400 AC/DC machine. The backside of the weld was also shielded with argon at a flow rate of 14 L/min. The GTAW process parameters included a voltage of 40 V, a current of 30 A, and a welding speed of 2 mm/s. The background current (Ib) of 50 A, the peak current (Ip) of 150 A, the welding speed of 2 mm/s, and the on-time of 50% were used as the process parameters for the pulsed current welding conditions in the PCGTAW process. The process parameters are summarized in Table 2. To minimize the formation of undesirable and detrimental phases in the weld metal and prevent weld joint distortion, the interpass temperature was strictly regulated between 120°C and 150°C. The primary objective was to achieve optimal fluidity and penetration, ensuring complete fusion between the base metal and ER309L filler metal while minimizing heat input to the weld pool and keeping it the same for continuous and pulsed current welding.

Table 1. The chemical composition of the base metal (BM) and filler (wt%)

	Ni	Cr	Fe	Ti	Al	Mo	Nb	Al	C	Si	Mn	Co	S	P
BM	Balance	19.1	3.22	2	1.33	0.9	0.38	1.33	0.07	0.06	0.06	0.05	0.004	0.003
	Fe	**Cr**	**Ni**	**Mn**	**Cu**	**Mo**	**Si**	**C**	**P**	-	-	-	-	-
Filer	Balance	24	13.5	2.1	0.27	0.2	0.4	0.02	0.001	-	-	-	-	-

[DOI: 10.22068/ijmse.3821]

Table 2. Welding process parameters

	GTAW	PCGTAW
Voltage (V)	40	40
Constant current (A)	30	-
I_p (A)	-	150
I_b (A)	-	50
On-time (%)	-	50
Speed (mm/s)	2	2
Shielding gas (L/min)	15	15
Back purged gas (L/min)	14	14

Three samples were prepared, as shown in Table 3.

Table 3. Samples

samples	process
No.1	GTAW of 25% pre-cold formed
No.2	GTAW of 50% pre-cold formed
No. 3	PCGTAW of 50% pre-cold formed

In the continuous current GTAW process, the heat input is calculated using Eq. 1, while in pulsed current GTAW it is calculated using the same equation after obtaining the average welding current (I_m) using Eq. 2.

$$\text{heat input} = \frac{EI\eta}{s} \quad (1)$$

$$I_m = \frac{I_p.t_p + I_b.t_b}{t_p + t_b} \quad (2)$$

Where E is the welding voltage (V); I is the welding current in the GTAW process and I_m is the average welding current in the PCGTAW process (A); s is the welding speed (mm/s); η is the process efficiency which is assumed to be 0.6 for GTAW process; I_p and I_b are the peak and base current in PCGTAW process (A), respectively, and t_p and t_b are the time of the pulse at peak and base current (s), respectively.

Regarding the parameters in both GTAW and PCGTAW processes and Eqs 1 and 2, the heat input in these two processes is similar and equal to 360 KJ/mm.

2.3. Pre-Cold Deformation Process

To investigate the effect of pre-cold deformation on the weldment properties, 25% and 50% reductions in thickness were applied by cold rolling using an appropriate lubricant. The latter amount of deformation is considered severe plastic deformation.

2.4. Microstructural Examination

To investigate microstructural evolution, the cross-section of the welded samples, consisting of the base metal, HAZ, and weld metal, was prepared by a conventional metallographic procedure, including sanding and polishing with alumina suspension. The samples were then etched for 60 seconds in a solution of 100 mL HCl, 5 mL H_2SO_4, and 5 g of $CuSO_4$ Optical microscopy (OM) and field emission scanning electron microscopy (FE-SEM) were performed with an LVSTD EDS analyzer.

Furthermore, X-ray diffraction (XRD) was performed with AW-XDM300 SSC 40 kV/30 mA machine using Cu Kα radiation (wavelength of 1.54 Å). The crystallite size in the weldments was determined using Scherer's formula (Eq. 3) [22].

$$\tau = \frac{k\lambda}{B.\cos\theta} \quad (3)$$

Where τ is the mean size of the crystallite, k is a dimensionless shape factor with a typical value of about 0.9, B is the peak width at half the maximum (FWHM), and θ is the Bragg angle.

2.5. Mechanical Investigation

Tensile testing and Vickers microhardness measurements were employed to evaluate the mechanical properties. Tensile samples, prepared according to ASTM E8 standard, were tested at a strain rate of 10^{-2} s^{-1} using a SANTAM instrument at room temperature. To evaluate the fracture characteristics, the fractured tensile samples were subjected to fractography using FE-SEM.

The Vickers cross-sectional hardness profile of the welded joints was determined using an applied load of 100 g for 20 seconds. Each hardness measurement was repeated three times to ensure accuracy, and the average values were reported.

3. RESULTS AND DISCUSSION

3.1. Microstructure

3.1.1. Base metal

The optical micrographs in Fig. 2 highlight the microstructural differences in Nimonic 80A under various cold-working conditions. Optical microscopy reveals a polygonal grain structure with a consistent distribution of secondary precipitates. The base metal of Nimonic 80A is characterized by a homogeneous microstructure with a solid solution strengthening phase inherent to high-temperature nickel-based alloys [16].

Fig. 2 (a) and (b) illustrate the microstructure of

[DOI: 10.22068/ijmse.3821]

the base metal following 25% and 50% cold working, respectively. Since the amount of cold deformation affects the shape of grains and not the size, no grain refinement was observed. Fig. 2 (b) also shows more twin boundaries due to a higher degree of cold deformation.

Fig. 3(a) demonstrates the morphology of the secondary phase in the base metal. Fig 3(b) and Table 4 show the EDS result of the phase, which is rich in Titanium and molybdenum.

Table 4. The EDS analysis quantitative results of phase A are shown in Figure 3

		Wt %	At %
Carbon	K Series	12.56	40.79
Titanium	K Series	47.71	38.87
Chromium	K Series	3.38	2.54
Cobalt	K Series	4.07	2.70
Nickel	K Series	7.70	5.12
Molybdenum	L Series	24.58	9.99

3.1.2. Heat affected zone (HAZ)

The optical micrographs in Fig. 4 illustrate the microstructural changes in the HAZ of Nimonic 80A for various welding and pre-cold-working conditions. Fig. 4(a), (b), and (c) show the HAZ of the sample with 25% cold working before GTAW, the HAZ of the 50% pre-cold-worked sample after GTAW, and the HAZ microstructure of the sample subjected to 50% cold working followed by PCGTAW. In the HAZ, distinct microstructural changes occur due to the thermal influence of the welding process. The grain size in the GTAWed 25% pre-cold-worked sample's HAZ is larger than that of the 50% pre-cold-worked sample, suggesting a lower dislocation density and less stored strain energy during welding. The combination of 50% cold working and the pulsed current welding technique results in the most refined grain structure among the samples.

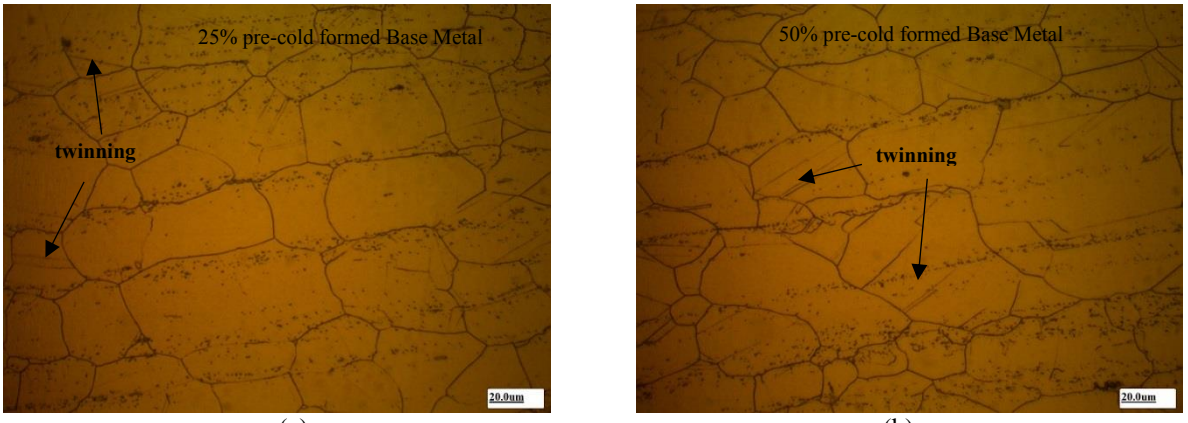

(a) (b)

Fig. 2. Optical microstructure of the base metal of Nimonic 80A in a) after 25% CW, b) after 50% CW

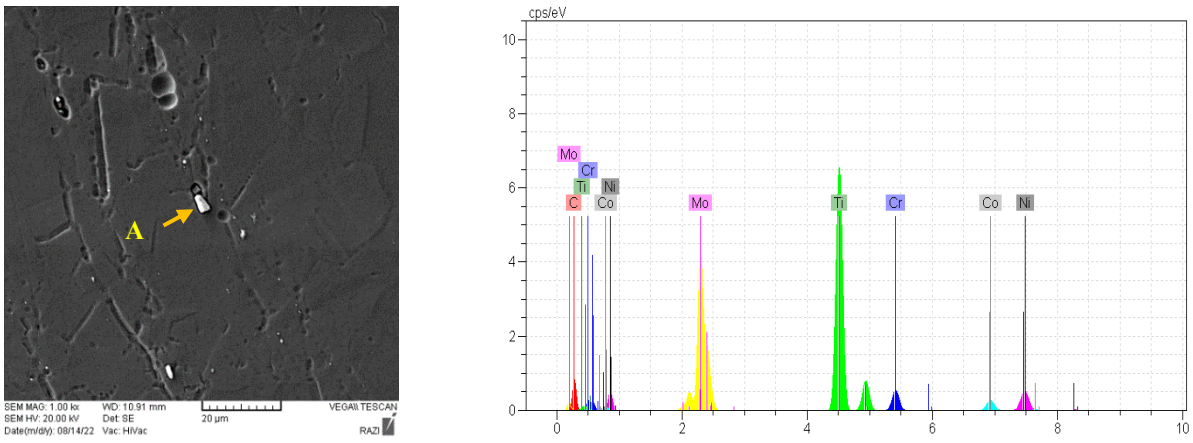

(a) (b)

Fig. 3. Secondary phase in base metal a) micrograph b) EDS spectrum result of phase A

[DOI: 10.22068/ijmse.3821]

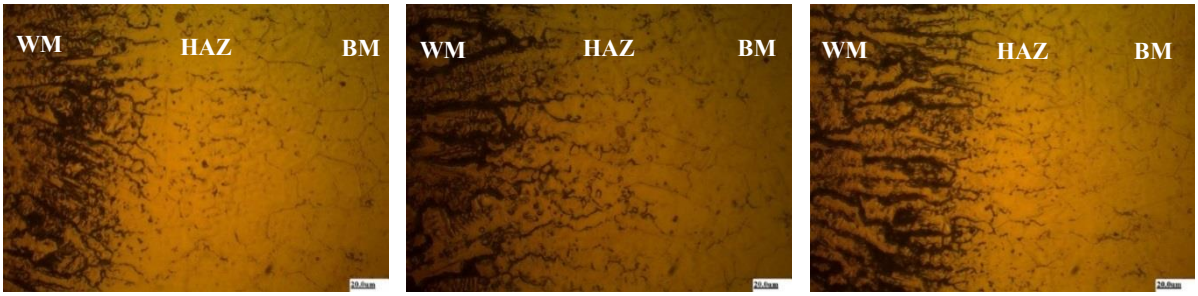

(a) (b) (c)

Fig. 4. Optical microstructure of the HAZ of Nimonic 80A in a) GTAW after 25% CW, b) GTAW after 50% CW, and c) PCGTAW after 50% CW

Despite the similar heat input in this study's GTAW and PCGTAW processes (see Section 2-2), the pulsed current welding process helps control heat input more effectively, reducing thermal gradients and promoting uniform grain refinement across the HAZ. The superior grain refinement in the HAZ of the PCGTAW-treated sample is expected to enhance the mechanical properties of the welded joint by improving its resistance to thermal and mechanical stress.

The HAZ experiences significant thermal exposure, leading to grain growth, dissolution of strengthening γ′ precipitates (Ni3Al), and potential carbide precipitation. The differences between 25% and 50% pre-cold-worked samples are primarily linked to the stored strain energy, which affects recrystallization kinetics. Higher pre-cold work results in a finer microstructure in the HAZ due to the enhanced nucleation of recrystallized grains upon heating, which suppresses grain coarsening [5, 23]. The superior refinement observed in the PCGTAW-treated HAZ is due to the better control over peak temperatures, reducing excessive grain growth while promoting recovery.

Fig. 5 presents the scanning electron microscopy (SEM) micrographs for three different samples of Nimonic 80A weldments: (a) the interface of Gas Tungsten Arc Welding (GTAW) with 25% cold work, (b) the interface of GTAW with 50% cold work, and (c) the interface of pulsed current GTAW (PCGTAW) with 50% cold work. In the sample with 25% pre-cold work, the SEM results show a relatively smooth transition across the interface between the base metal and the weld zone, which indicates a uniform elemental distribution.

In contrast, the higher degree of cold work affects the microstructural transitions during welding, as expected in the sample with 50% pre-cold work. As demonstrated by [24, 25], the interface between the base metal and the weld metal in the highly pre-cold-worked samples shows more pronounced features, such as strain bands and dislocation tangles, indicative of higher internal stress and localized deformation. The increased dislocation density due to the higher cold work leads to enhanced grain refinement, making the microstructure finer.

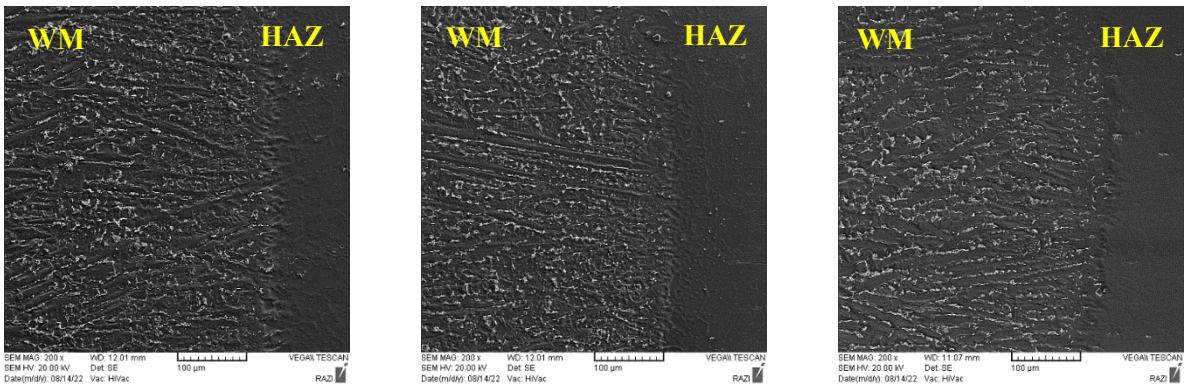

(a) (b) (c)

Fig. 5. SEM micrographs of WM/HAZ interfaces of different samples: a) GTAWed 25% CW, b) GTAWed 50% CW, c) PCGTAWed 50% CW

[DOI: 10.22068/ijmse.3821]

The weld metal/base metal interface in the PCGTAW sample shows smoother transitions with fewer irregularities compared to the sample welded using continuous GTAW.

3.1.3. Weld metal

Fig. 6 presents the optical micrographs of the WZ of Nimonic 80A for three different welding conditions. In Fig. 6(a), the sample with 25% pre-cold working subjected to GTAW reveals a coarse dendritic structure in the weld zone, typical of fusion welds. Fig. 6(b) shows the WZ of the sample that was 50% pre-cold-worked before undergoing GTAW. Fig. 6(c) shows the microstructure of the WZ of the sample that underwent 50% pre-cold working followed by pulsed current GTAW. As seen from Fig 6(a) and 6(b), the dendritic structures of the WM in GTAWed samples are almost the same in size regardless of the amount of pre-cold work, as the WM exhibits a solidification microstructure which does not depend on pre-cold work condition but the heating regime and cooling rate. On the other hand, as Fig 6(c) reveals, the PCGTAW process results in a significantly refined dendritic structure despite the same heat input as the GTAW process, as previously calculated in section 2-2. This evidence may be interpreted in terms of the pulsating nature of the incident heat in PCGTAW, which can increase the cooling rate compared to that in GTAW. The WZ exhibits a dendritic austenitic structure due to the rapid solidification of the molten weld pool. The microsegregation of alloying elements such as Cr, Ti, and Mo into interdendritic regions is typical in nickel-based superalloys [2, 3]. The application of PCGTAW resulted in finer dendritic structures than continuous GTAW, a phenomenon attributable to the higher cooling rates induced by pulsed current welding [13]. The pulsating heat input promotes heterogeneous nucleation and reduces solute redistribution, thereby refining the microstructure and mitigating the formation of secondary brittle phases such as carbide precipitates or Laves phases [15, 16].

Fig. 7 presents the scanning electron microscopy (SEM) images for three different samples of Nimonic 80A weldments: (a) WM (weld metal) of GTAW with 25% pre-cold work, (b) WM of GTAW with 50% pre-cold work, and (c) WM of PCGTAW with 50% pre-cold work. The WZ also exhibits a relatively uniform microstructure with fewer signs of defects or irregularities. Using pulsed current GTAW (PCGTAW) with 50% cold work, as shown in Fig. 7(c), produces a more refined microstructure in the weld metal. Fig 7(d) and Table 5 show the chemical composition of phase A, which is specified in Fig. 7(a) as the interdendritic phase. Such interdendritic phases are rich in Ti, Mo, and Cr.

Table 5. The EDS analysis quantitative results of phase A are shown in Figure 7

		Wt %	At %
Carbon	K Series	3.31	14.24
Silicon	K Series	0.35	0.68
Titanium	K Series	14.58	17.11
Chromium	K Series	16.62	17.48
Iron	K Series	9.24	9.05
Cobalt	K Series	5.06	4.70
Nickel	K Series	20.82	19.40
Niobium	L Series	19.73	11.62
Molybdenum	L Series	10.07	5.74

The microstructure of the WM primarily consists of an austenitic dendritic matrix, with interdendritic precipitates rich in Ti, Mo, and Cr (as shown in the SEM-EDS analysis in Fig. 7 and Table 5). These precipitates contribute to the strengthening of the WM by impeding dislocation motion.

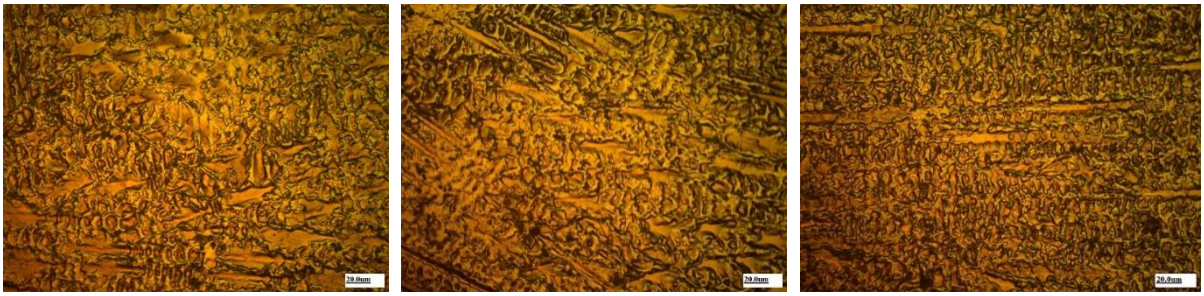

(a) (b) (c)

Fig. 6. Optical microstructure of the WZ of Nimonic 80A in a) GTAW after 25% CW, b) GTAW after 50% CW, and c) PCGTAW sample

[DOI: 10.22068/ijmse.3821]

However, variations in dendritic size and distribution between different welding conditions influence the local stress-strain response, leading to differences in tensile strength.

The PCGTAW sample exhibits a more uniform dendritic arrangement, contributing to improved mechanical performance compared to GTAW samples. While the overall heat input in both GTAW and PCGTAW processes was maintained at 360 KJ/mm (calculated in Section 2.2), the pulsed current process facilitates better heat distribution and reduced peak temperatures, minimising excessive grain coarsening.

3.1.4. XRD results

The results of XRD analysis are shown in Fig. 8. The austenitic matrix is characterized by prominent peaks at approximately the 2θ of 43.61°, 50.80°, 74.70°, and 90.60°, corresponding to (111), (200), (220) and (311) planes, respectively. For the 25% cold-worked sample, the (111) peak intensity is slightly lower compared to the 50% cold-worked sample (545.3 cts vs. 546.2 cts). The FWHM for this peak remains constant at 0.54°, indicating similar crystallite sizes and internal strain in both samples. The Ni_3Al phase shows peaks at 2θ of 35.21°, 43.6°, and 50.70°, corresponding to (110), (111), and (200) planes. The GTAWed sample with 25% pre-cold work displays the sharpest peaks with the smallest full width at half maximum (FWHM), indicating larger grain sizes and less lattice strain.

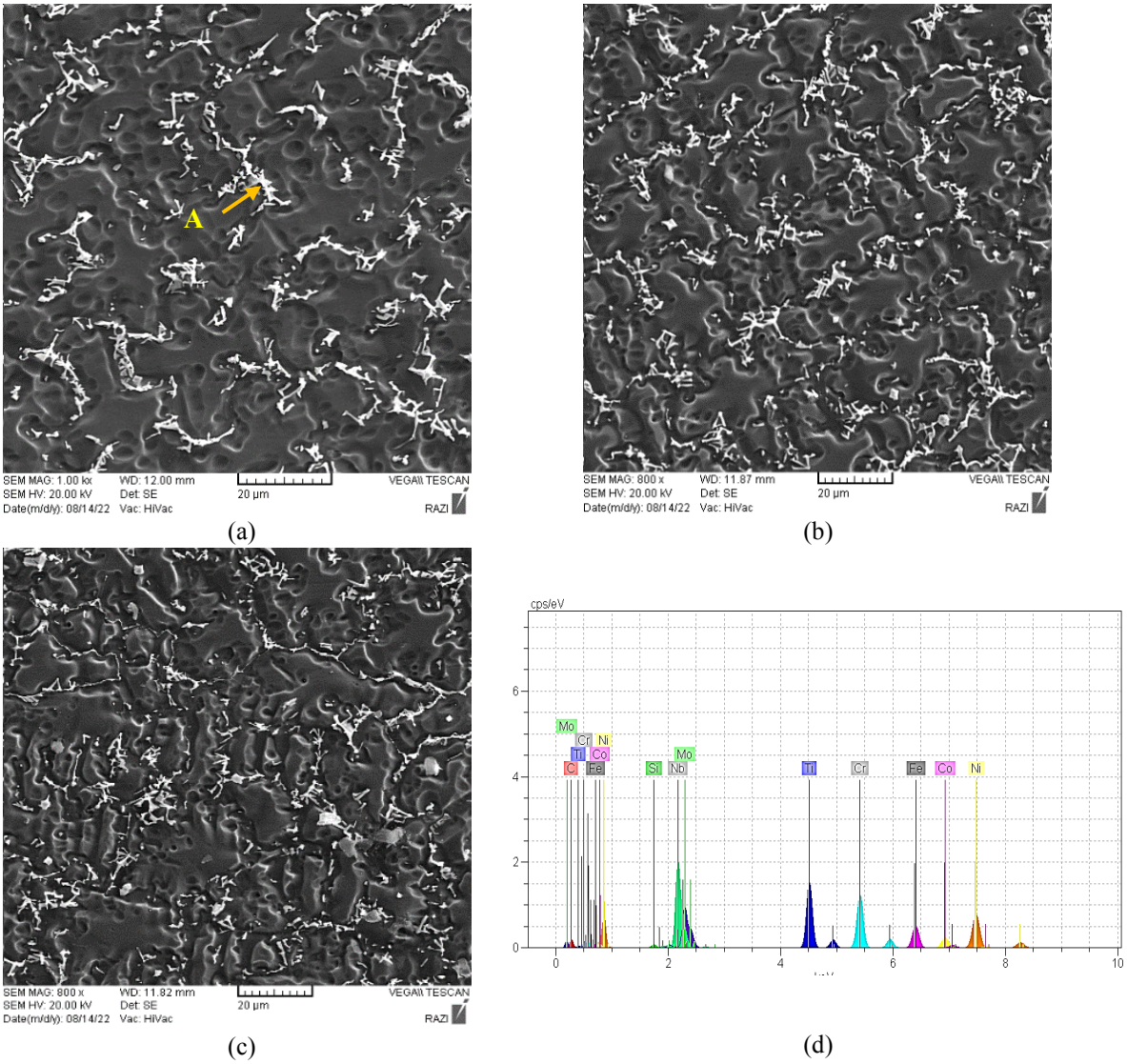

Fig. 7. SEM of GTAW-weldment of different samples, a) Weld Metal (WM) of GTAW 25% CW, b) WM of GTAW 50% CW and c) WM of PCGTAW, d)EDS spectrum result of phase A

[DOI: 10.22068/ijmse.3821]

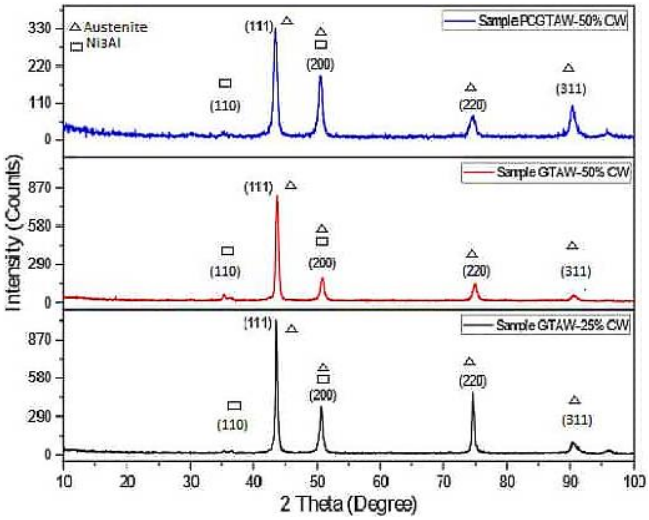

Fig. 8. XRD analysis of Nimonic 80A weldments of GTAW and PCGTAW samples

GTAWed sample with 50% CW shows broader peaks compared to the GTAW sample with 25% CW, suggesting smaller grain sizes and increased lattice strain due to the higher degree of cold working. Also, the PCGTAW sample exhibits the broadest peaks among the three samples, indicating the smallest grain sizes. The FWHM values for the Ni_3Al peaks are also slightly narrower in the 50% cold-worked sample, indicating a potential reduction in grain refinement with higher cold work. No significant peak shifts are observed between the samples, suggesting that the lattice parameters remain relatively constant despite the different processing conditions.

3.2. Mechanical Properties

3.2.1. Tensile test

In the tensile properties of Nimonic 80A samples welded via GTAW, notable differences emerged between the pre-cold-worked (CW) samples. The sample with 25% pre-cold worked before welding exhibited lower tensile strength and higher elongation than those with 50% cold work. The fracture of the welded samples consistently occurred within the WZ in a ductile mode, typical for austenitic welds, especially with less intense pre-cold work. The yield and tensile strength of different samples are compared in Fig. 9.

In comparison, the 50% pre-cold-worked sample, 50% cold-worked before GTAW, demonstrated higher tensile strength due to the greater degree of cold work, resulting in more strain hardening. PCGTAW sample, which was also 50% cold-worked but underwent PCGTAW with a background current of 50A and a pulse current of 150 A, showed the highest tensile strength among the three samples. The combination of 50% cold work and the controlled heat input from the PCGTAW process resulted in a finer grain structure in the weld zone, enhancing its mechanical properties.

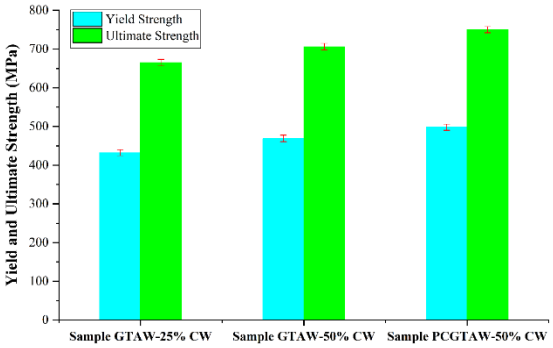

Fig. 9. Comparison of yield and tensile strength of GTAW samples with 25% and 50% pre-cold work levels and the PCGTAW sample with pulsed current welding parameters

Despite the higher strength, the ductility of the PCGTAW sample was comparable to the 50% pre-cold-worked sample, as the benefits of grain refinement were offset by the thermal stresses induced by the pulsed current welding. The stress-strain curves of these samples, highlighting the differences between the 25% and 50% cold-worked GTAW samples and the PCGTAW sample, are shown in Fig. 10.

Tensile testing revealed fractures within the WZ, followed by a ductile failure mode. The fracture mechanism is governed by the formation and coalescence of microvoids, which are influenced by the weld metal's microstructure. The PCGTAW

[DOI: 10.22068/ijmse.3821]

sample, with a refined grain structure, exhibited the highest strength (766 MPa), a result consistent with the Hall-Petch relationship, where smaller grain sizes enhance yield strength [26]. This aligns with studies reporting similar enhancements in mechanical performance with refined weld microstructures in nickel-based superalloys [10].

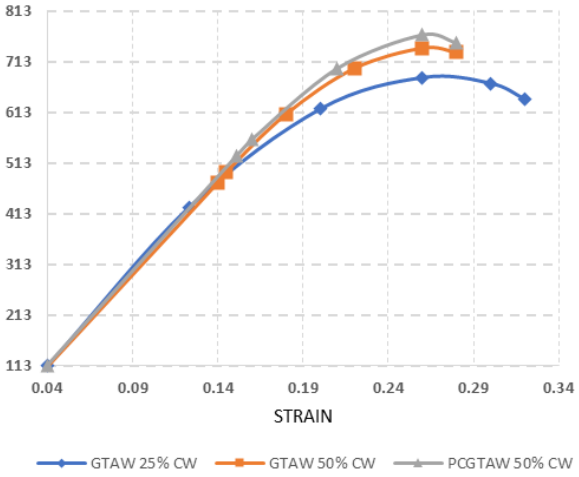

Fig. 10. stress-strain curves of GTAW samples with two different pre-cold work levels (25% and 50%) and the PCGTAW sample

Therefore, the primary difference in WM microstructure between samples is attributed to the variation in the welding process parameters, particularly the use of continuous versus pulsed current GTAW. As demonstrated in the microstructural analysis (Fig. 6 and Fig. 7), the pre-cold-worked samples (especially those with 50% cold work) exhibit a more refined microstructure in the WM when welded using Pulsed Current GTAW (PCGTAW). The finer grain structure in the PCGTAW samples, compared to the coarser dendritic structure in the conventional GTAW samples, improves mechanical properties, including tensile strength. The pulsed nature of PCGTAW results in intermittent heating and cooling cycles, promoting grain refinement due to an increased cooling rate compared to continuous GTAW.

3.2.2. Microhardness

Fig. 11 illustrates the evolution of microhardness in the samples that were subjected to different pre-cold-worked levels and welding conditions. The 50% cold-worked base metal exhibits higher hardness than the base metal with 25% cold-work. An increase in the degree of cold work is expected to increase the initial dislocation density since cold working typically increases the dislocation density in the material, which leads to strain hardening [23]. This phenomenon has also been observed in Nimonic 80A samples [4]. However, the thermal cycle of the welding process, particularly in the HAZ and WZ, alters the microstructure through recrystallization and grain growth, potentially reducing hardness in these regions.

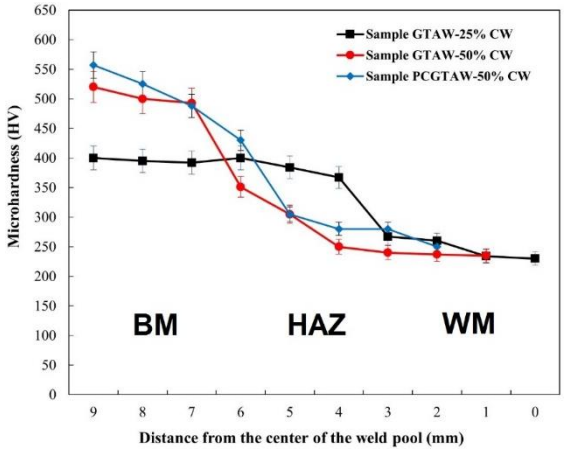

Fig. 11. Microhardness evolution of Nimonic 80A samples with 25% and 50% pre-cold work levels, comparing GTAW and PCGTAW processes

For the 25% cold-worked sample, the welding process results in the melting and solidification of the WZ, which leads to substantial microstructural changes. During this process, the cold work-induced strain hardening is annihilated, and the WZ develops a softer, more equiaxed grain structure. Additionally, the filler metal is much softer than the base metal. Consequently, the microhardness in the WZ decreases significantly compared to the base material. This results in a decrease in microhardness compared to the base material, though it is still higher than in the WZ due to the retention of some cold work-induced hardness. In contrast, the 50% cold-worked sample exhibits a more pronounced reduction in microhardness in both the WZ and HAZ. The higher pre-cold−work introduces greater strain energy into the material, intensifying recovery and recrystallization processes during welding. As the WZ undergoes melting and solidification, the loss of cold-work-induced dislocation density results in a greater decrease in hardness compared to the 25% cold-worked sample.

When comparing these two samples with the 50% cold-worked PCGTAW sample, which was welded using a background current of 50 A and a

[DOI: 10.22068/ijmse.3821]

pulse current of 150 A, the pulsed current process introduces additional microstructural control. The PCGTAW process allows for better regulation of heat input, leading to more refined microstructures in the WZ and HAZ. As a result, the hardness in the WZ of the PCGTAW sample is expected to be higher than that of the conventionally welded 50% cold-worked sample, as the pulsed current reduces the extent of grain growth and recrystallization. However, the overall trend of decreased microhardness due to the loss of cold-work-induced hardness still holds, with the PCGTAW sample showing a less drastic reduction in hardness than the 50% cold-worked GTAW sample. The HAZ in the PCGTAW sample similarly benefits from the controlled heat input, resulting in finer grains and less pronounced recovery compared to the standard GTAW process, maintaining relatively higher hardness in this region. Microhardness measurements confirmed a significant reduction in hardness in the WZ and HAZ compared to the BM. This reduction was more pronounced in the 50% cold-worked sample due to the loss of strain-hardening effects. However, the PCGTAW sample retained higher hardness, likely due to the refined dendritic microstructure and the inhibition of excessive softening through controlled heat input. These results are consistent with findings on nickel alloys, where pulsed current welding reduces grain coarsening and enhances microhardness retention [14].

3.2.3. Fractography

Fig. 12 presents the fractography of tensile samples for three different weldments: (a) GTAW with 25% pre-cold work, (b) GTAW with 50% pre-cold work, and (c) PCGTAW with 50% pre-cold work. The fractographic analysis provides a detailed understanding of the failure modes in these tensile samples, revealing the characteristic features of ductile fracture across all samples. Since all tensile samples failed in the weld metal, the characteristics of the fracture surfaces are mainly influenced by the welding process rather than the base metal condition. As can be seen in Fig 12 (a), (b), and (c), all surfaces show the characteristics of a ductile fracture consisting of microvoids and dimples.

In the 25% cold-work GTAWed sample, Fig 12 (a), the dimples appear uniform in size and distribution, suggesting that the material underwent a more homogeneous stress distribution and plastic deformation before failure. Microvoid coalescence, where smaller voids merge to form larger dimples, is also observed, confirming the material's ability to absorb significant energy before fracturing. The overall fracture surface in this sample is smooth and consistent, with no evidence of localized stress concentrations, highlighting a uniform ductile failure mechanism. The 50% cold work GTAWed sample, Fig 12 (b), exhibits a more complex and varied fracture morphology. Additionally, the coalescence of microvoids is more pronounced, resulting in larger dimples due to the elevated strain energy. The fracture surface is more rugged and uneven, with potential signs of secondary cracks or shear bands in some regions.

Finally, the PCGTAWed sample with 50% pre-cold work, Fig 12 (c), presents a fracture surface that is more refined compared to the continuous GTAWed samples. The pulsed current technique in PCGTAW helps to localize heat during welding, resulting in a more controlled stress distribution across the weldment.

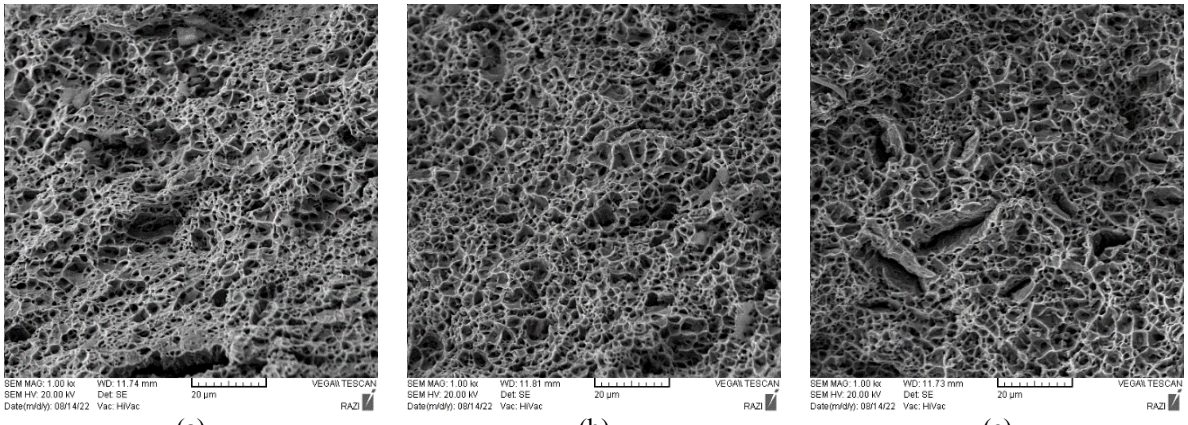

(a) (b) (c)

Fig. 12. Fractography of tensile failure samples a) GTAW 25% CW and b) GTAW 50% CW c) PCGTAW 50% CW

[DOI: 10.22068/ijmse.3821]

The fractography of the PCGTAWed sample still displays the characteristic ductile fracture features, with microvoids and dimples present. However, the overall fracture morphology appears smoother than in the 50% cold work GTAWed sample. Using PCGTAWed appears to mitigate some of the more pronounced effects of higher cold work, leading to a more uniform dimple distribution and a less rugged fracture surface.

The fractographic analysis (Fig. 12) confirms that all tensile failures occurred within the WM and exhibited ductile fracture characteristics, with microvoids and dimples being predominant. However, differences in dimple morphology suggest that the PCGTAW sample experienced a more uniform stress distribution during deformation, whereas the GTAW samples with 50% cold work displayed localized strain accumulation, which may have contributed to the slight variations in tensile strength.

4. CONCLUSIONS

This study investigated the microstructural and mechanical behavior of Nimonic 80A superalloy weldments under different pre-cold working conditions (25% and 50%) using conventional GTAW and PCGTAW. The key findings are as follows:

1- The welding process induced significant microstructural changes, particularly in the HAZ and WZ. These changes were most pronounced in the 50% cold work sample. In comparison, the 25% cold work sample exhibited a smoother transition between the base metal and WZ. The PCGTAW samples exhibit a more refined dendritic structure despite having the same heat input as conventional GTAW. The improved grain refinement in the PCGTAW process resulted from controlled thermal cycling and enhanced cooling rates.

2- XRD analysis showed that the microstructure consists of an austenitic matrix strengthened by the Ni_3Al phase. The GTAWed sample with 25% pre-cold work displays the sharpest peaks with the smallest full width at half maximum (FWHM), indicating larger grain sizes and less lattice strain. The PCGTAW sample displayed broader peaks, indicating smaller grain sizes and a more refined microstructure compared to GTAWed samples. No significant peak shifts are observed between the samples, suggesting that the lattice parameters remain relatively constant despite the different processing conditions.

3- The tensile test results confirmed that all samples fractured within the WZ, exhibiting a ductile failure mode. The PCGTAW sample demonstrated the highest tensile strength (766 MPa), emphasizing the benefits of pulsed current welding in enhancing mechanical performance.

4- All samples exhibited ductile fracture characteristics, with microvoids and dimples present in the fracture surfaces. The PCGTAW sample showed a more refined and uniform dimple structure, suggesting improved stress distribution and enhanced weld quality.

5- While the base metal's hardness increased with pre-cold working, the WZ and HAZ exhibited reduced hardness levels due to welding-induced microstructural changes. However, the PCGTAW sample retained a higher hardness compared to GTAWed samples, indicating better preservation of mechanical integrity.

DECLARATIONS

Conflict of interest the authors declare that they have no conflict of interest.

FUNDING

The authors did not receive support from any organization for the submitted work.

AVAILABILITY OF DATA AND MATERIALS

The data that support the findings of this study are available from the corresponding author upon reasonable request.

AUTHORS' CONTRIBUTIONS

The first author: Results, Writing- Original Draft. Second author: Conceptualization, Methodology, Supervision, Validation, Writing-Reviewing and Editing and third author: Supervision, Validation, Writing-Reviewing and Editing. Fourth author: Supervision, Data curation.

ACKNOWLEDGEMENTS

None.

[DOI: 10.22068/ijmse.3821]

REFERENCES

[1]. Luijan, J., Surin, P. and Eidhed, K., "Investigation of ER308L and ER309L filler wires on dissimilar metals between carbon steel and 3CR12 ferritic stainless steel by GTAW through boiler fabrication in a sugar factory". Mater. Res. Express., 2023, 10, 126501.

[2]. Janaki Ram, G. D., Venugopal Reddy, A., Prasad Rao, K. and Madhusudhan Reddy, G., "Control of Laves phase in Inconel 718 GTA welds with current pulsing". Sci. Technol. Weld. Join., 2004, 9, 390-398.

[3]. Manikandan, S., Sivakumar, D., Prasad Rao, K. and Kamaraj, M., "Effect of weld cooling rate on Laves phase formation in Inconel 718 fusion zone". J. Mater. Process. Technol., 2014, 214, 358-364.

[4]. Voice, W. E. and Faulkner, R. G., "Carbide stability in Nimonic 80A alloy". Metall. Trans. A., 1985, 16, 511-520.

[5]. Bombac, D., Brojan, M., Tercelj, M., Turk, R., "Response to hot deformation conditions and microstructure development of Nimonic 80A superalloy". Mater. Manuf. Process., 2009, 24, 644-648.

[6]. Kangazian, J., Sayyar, N., Shamanian, M., "Influence of microstructural features on the mechanical behavior of Incoloy 825 welds" Metallogr. Microstruct. Anal.,2017, 6, 190-199.

[7]. Sabry, I., Hewidy A. M., "Multi-Weld Quality Optimization of Gas Tungsten Arc Welding for Aluminium 6061 using the Grey Relation Analysis-Based Taguchi Method". J. Adv. Res. Appl. Sci. Eng. Technol., 2023, 36, 26-42.

[8]. Lieth, H. M., Jabbar, M. A., Jassim, R. J. and Al-Sabur, R., "Optimize the corrosion behavior of AISI 204Cu stainless steel in different environments under previous cold working and welding". Metall. Res. Technol., 2023, 120, 415.

[9]. Tian, S., Xu F., Zhang, G., Saifan, A., Saleh, B. and Li, X., "Influence of post-weld heat treatment on microstructure and toughness properties of 13MnNiMoR high strength low alloy steel weld joint". Materials, 2021, 14, 5336.

[10]. Manikandan, M., Arivazhagan, N., Rao, M. N. and Reddy, G. M., "Microstructure and mechanical properties of alloy C-276 weldments fabricated by continuous and pulsed current gas tungsten arc welding techniques". J. Manuf. Process., 2014, 16, 563-572.

[11]. Srikanth, A. and Manikandan, M., "Development of welding technique to avoid the sensitization in the alloy 600 by conventional Gas Tungsten Arc Welding method". J. Manuf. Process., 2017, 30, 452-466.

[12]. Manikandan, M., Arivazhagan, N., Rao, M. N. and Madhusudhan Reddy, G., "Improvement of microstructure and mechanical behavior of gas tungsten arc weldments of alloy C-276 by current pulsing". Acta Metall. Sin. -Engl. Lett., 2015, 28, 208-215.

[13]. Subramani, P., Manikandan, M., "Development of gas tungsten arc welding using current pulsing technique to preclude chromium carbide precipitation in aerospace-grade alloy 80A". Int. J. Miner. Metall. Mater., 2019, 26, 210-221.

[14]. Arivarasu, M., Ramkumar Kasinath, D., and Natarajan, A., "Effect of continuous and pulsed current on the metallurgical and mechanical properties of gas tungsten arc welded AISI 4340 aeronautical and AISI 304 L austenitic stainless steel dissimilar joints". Mat. Res., 2015, 18, 59-77.

[15]. Pasupathi, S., Sathishkumar, M., Anbarasan, N., Naiju, C., Manoharan, M., and Jerome, S., "Studies on Metallurgical and Mechanical Properties of Plasma Arc Welded Aerospace 80A Grade Alloy", SAE Technical Paper, 2020, 0148-7191.

[16]. Zhang, H., Huang, C., Guan, Z., Li, J., Liu, Y., Chen, R. and Wang, Q., "Effects of the electron beam welding process on the microstructure, tensile, fatigue and fracture properties of nickel alloy nimonic 80A". J. Mater. Eng. Perform., 2018, 27, 89-98.

[17]. Atapek, Ş. H., Tümer, M., Çelikkol, E., Kısasöz, A., Kerimak, M. Z., "Microstructural, mechanical and corrosion behavior of UNS S31803/Hastelloy C-276 dissimilar metal welds" CIRP. J. Manuf. Sci. Technol., 2023, 40, 129-141.

[18]. Keienburg, K. H., Deblon, B., "Refurbishing procedures for blades of large stationary gas turbines". Mater. Sci. Technol., 1985,

[DOI: 10.22068/ijmse.3821]

1, 620-628.
[19]. Xu, Y., Yang, C., Ran, Q., Hu, P., Xiao, X., Cao, X. and Jia, G., "Microstructure evolution and stress-rupture properties of Nimonic 80A after various heat treatments". Mater. Des., 2013, 47, 218-226.
[20]. Ramkumar, K. D., Krishnan, S. R., Ramanand, R., Logesh, S., Satyandas, T., Ameer, A. and Arivazhagan, N., "Structure–property relationships of PCGTA welds of Inconel X750 in as-welded and post-weld heat treated conditions—A comparative study". J. Manuf. Process., 2015, 20, 1-14.
[21]. Subramani, P., Arivazhagan, N., Selvaraj, S. K., Mancin, S. and Manikandan, M., "Influence of hot corrosion on pulsed current gas tungsten arc weldment of aerospace-grade 80A alloy exposed to high temperature aggressive environment" Int. J. Thermofluids., 2022, 14, 100148.
[22]. Sandhu, K. S., Chatha, S. S. and Singh, H., "Effect of Crystallite Size on Mechanical Properties of Friction Stir Welded Al-Mg-Si Alloy". Int. J. Surf. Eng. Interdiscip. Mater. Sci., 2016, 6, 26-31.
[23]. Callister, W. D., Rethwisch, D. G., Materials science and engineering: an introduction, John wiley & sons, ISBN: 978-1-119-40549-8, 10th ed., 2018, 180-208.
[24]. Wang, Y., Zhang, W., Wang, Y., Lim, Y. C., Yu, X. and Feng, Z., "Experimental evaluation of localized creep deformation in grade 91 steel weldments". Mater. Sci. Eng. A, 2021, 799, 140356.
[25]. Yang, Q., Zhang, W., Yin, P., Wang, B., Chang, L. and Zhou, C., "Deformation and microregion fracture mechanisms in type 316L welded joint under isothermal and thermo-mechanical fatigue loadings". Mater. Sci. Eng. A, 2024, 916,147338.
[26]. Hall, E. O., "The deformation and ageing of mild steel: III discussion of results" Proc. Phys. Soc., 1951, 64, 747.

[DOI: 10.22068/ijmse.3821]